



Tumor-associated macrophages expressing galectin-9 identify immunoevasive subtype muscle-invasive bladder cancer with poor prognosis but favorable adjuvant chemotherapeutic response

Yangyang Qi¹ · Yuan Chang² · Zewei Wang³ · Lingli Chen⁴ · Yunyi Kong⁵ · Peipei Zhang⁶ · Zheng Liu² · Quan Zhou⁷ · Yifan Chen¹ · Jiajun Wang³ · Qi Bai³ · Yu Xia³ · Li Liu³ · Yu Zhu² · Le Xu⁸ · Bo Dai² · Jianming Guo³ · Yiwei Wang⁹ · Jiejie Xu⁷ · Weijuan Zhang¹

Received: 2 April 2019 / Accepted: 7 November 2019 / Published online: 12 November 2019
© Springer-Verlag GmbH Germany, part of Springer Nature 2019

Abstract

Purpose Tumor-associated macrophages (TAMs) exist as heterogeneous subsets and have dichotomous roles in cancer-immune evasion. This study aims to assess the clinical effects of Galectin-9⁺ tumor-associated macrophages (Gal-9⁺TAMs) in muscle-invasive bladder cancer (MIBC).

Experimental design We identified Gal-9⁺TAMs by immunohistochemistry (IHC) analysis of a tumor microarray (TMA) ($n = 141$) from the Zhongshan Hospital and by flow cytometric analysis of tumor specimens ($n = 20$) from the Shanghai Cancer Center. The survival benefit of platinum-based chemotherapy in this subpopulation was evaluated. The effect of the tumor-immune microenvironment with different percentages of Gal-9⁺TAMs was explored.

Results The frequency of Gal-9⁺TAMs increased with tumor stage and grade. Gal-9⁺TAMs predicted poor overall survival (OS) and recurrence-free survival (RFS) and were better than Gal-9⁻TAMs and TAMs to discriminate prognostic groups. In univariate and multivariate Cox regression analyses, patients with high percentages of Gal-9⁺TAMs showed the prominent survival benefit after receiving adjuvant chemotherapy (ACT). High Gal-9⁺TAM infiltration correlated with increasing numbers of regulatory T cells (Tregs) and mast cells and decreasing numbers of CD8⁺T and dendritic cells (DCs). Dense infiltration of Gal-9⁺TAMs was related to reduced cytotoxic molecules, enhanced immune checkpoints or immunosuppressive cytokines expressed by immune cells, as well as active proliferation of tumor cells. Additionally, the subpopulation accumulated was strongly associated with PD-1⁺TIM-3⁺CD8⁺T cells.

Conclusions Gal-9⁺TAMs predicted OS and RFS and response to ACT in MIBC patients. High Gal-9⁺TAMs were associated with a pro-tumor immune contexture concomitant with T cell exhaustion.

Keywords Galectin-9⁺ tumor-associated macrophages · Muscle-invasive bladder cancer · Adjuvant chemotherapy · Immune contexture

Parts of this paper were presented at the 17th International Congress of Immunology, 19–23 October 2019, Beijing, China, and published as an abstract in the European Journal of Immunology [1].

Yangyang Qi, Yuan Chang, Zewei Wang and Lingli Chen contributed equally to this work.

Electronic supplementary material The online version of this article (<https://doi.org/10.1007/s00262-019-02429-2>) contains supplementary material, which is available to authorized users.

Extended author information available on the last page of the article

Abbreviations

ACT	Adjuvant chemotherapy
AJCC	American Joint Committee on Cancer
AP	Alkaline phosphatase
DAB	Diaminobenzidine
DBSS	Dulbecco's balanced salt solution
FCM	Flow cytometry
Gal-9 ⁺ TAMs	Galectin-9 ⁺ tumor-associated macrophages
Gal-9 ⁻ TAMs	Galectin-9 ⁻ tumor-associated macrophages
GZMB	Granzyme B
HCl	Hydrochloric acid
HR	Hazard ratio
HRP	Horseradish peroxidase
ICIs	Immune checkpoint inhibitors

LVI	Lymphovascular invasion
MIBC	Muscle-invasive bladder cancer
PRF1	Perforin 1
RFS	Recurrence-free survival
TAMs	Tumor-associated macrophages
TIGIT	T-cell Ig and ITIM domain
TMA	Tissue microarray

Introduction

Approximately 0.4 million new cases of bladder cancer occur annually, one-fourth of which are muscle-invasive bladder cancer (MIBC) or metastatic bladder cancer. MIBC has a poor prognosis with a 5-year survival rate lower than 50% [2]. Adjuvant chemotherapy (ACT) has a potential therapeutic benefit for patients with advanced stage disease [3]. Furthermore, immune-checkpoint inhibitors (ICIs) have become an effective therapeutic option [4]. However, near-universal chemo-resistance [5] and low percentage (20%) of participating patients [6] who exhibit durable responses to ICIs have led to extensive efforts to detect more feasible predictive biomarkers to improve the response rate of curative treatments.

The presence of macrophages is related to unfavorable outcomes in various human cancers, including bladder cancer [7]. Although TAMs are primarily found as a protumorigenic M2 phenotype [8, 9], high infiltration of M1 macrophages correlates with improved clinical outcomes in solid tumors [10]. Nevertheless, a study discovered that TAMs isolated from pancreatic ductal adenocarcinoma co-expressed IFN-induced chemokines and high levels of IL-10 [11], suggesting that TAMs may concurrently exhibit both M1 and M2 characteristics. Therefore, conventional M1 or M2 macrophages might not accurately indicate the prognosis of all patients. A more specific subtype of macrophages that can predict prognosis and therapeutic response is needed for an understanding of the precise role of macrophages in cancers. Additionally, previous studies have simply focused on the relationship between prognosis and the infiltration of specific macrophages without comprehensively considering the microenvironment, such as interaction among tumor cells, other immune cells and the whole tumor ecosystem [4]. Indeed, Fridman et al. [12] emphasized that the context-specific nature of infiltrating immune cells could affect the clinical outcomes of patients, implying that further exploration is required to identify the dynamic changes in the microenvironment.

In recent years, tumor-derived galectin-9, which can predict favorable outcomes in most solid tumors [13–16], including bladder urothelial carcinoma [17], has attracted attention. However, researchers to date have increasingly focused on the function of galectin-9 expressed by

Fig. 1 Flow cytometric analysis and immunohistochemistry staining confirm the presence of galectin-9⁺TAMs in MIBC patients. **a** Representative flow cytometric plots of galectin-9⁺CD45⁺CD68⁺ macrophages. **b** Percentage of Gal-9⁺TAMs in tumor and peritumor tissues ($n=6$), as based on the paired *t* test. **c** Representative images of double staining for galectin-9 (brown) and macrophages (CD68, blue); 200 \times magnification; scale bar, 100 μ m; 400 \times magnification; scale bar, 50 μ m. **d** Proportion of Gal-9⁺ and Gal-9⁻TAMs. **e** Frequency of Gal-9⁺TAMs among different tumor stages and **f** grades observed by FCM (left) and IHC (right)

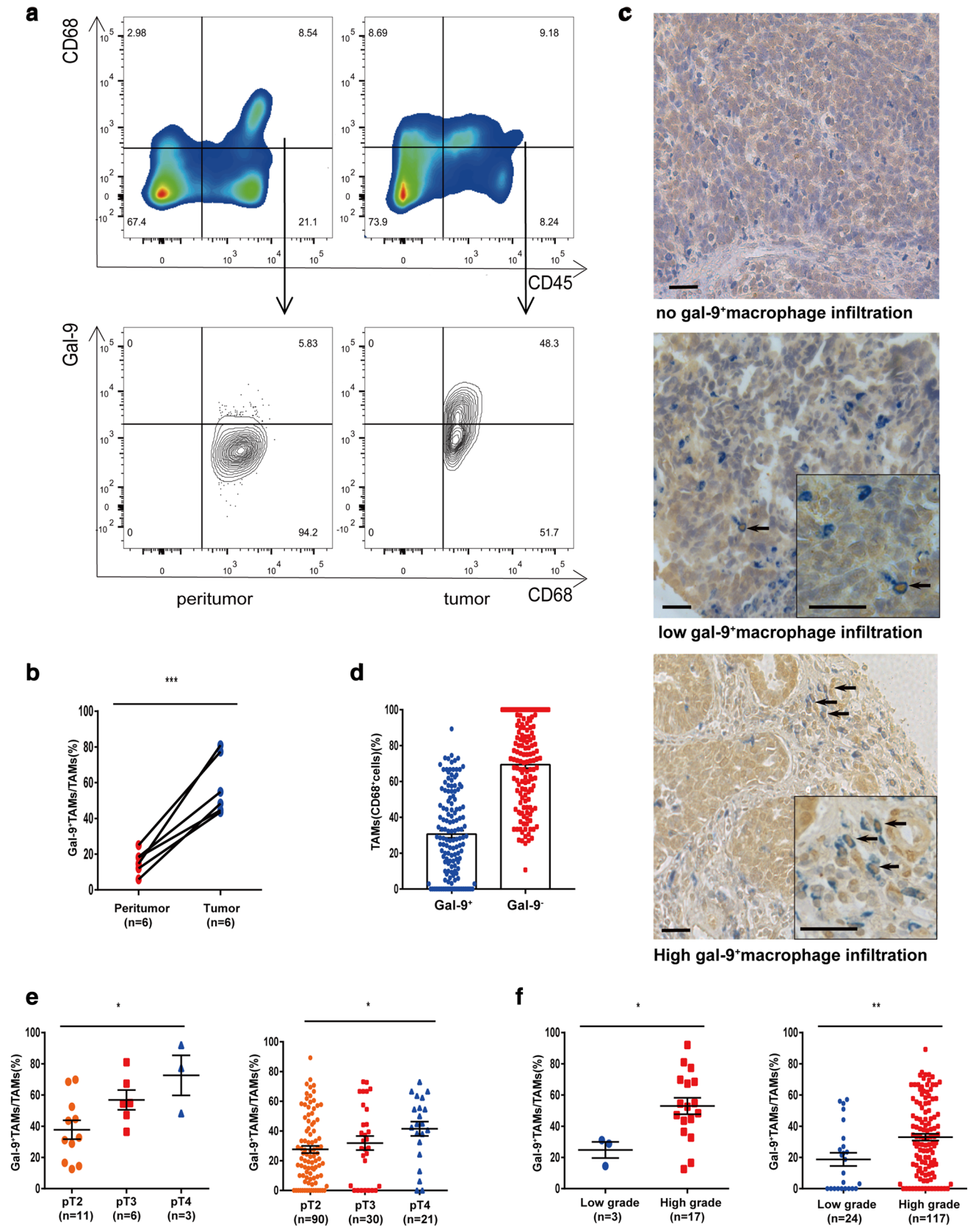
macrophages. For example, Li et al. [18] found that patients with high infiltration of galectin-9⁺ Kupffer cells (KCs) and TIM-3⁺ T cells had a poor prognosis. These HBV-associated hepatocellular carcinoma patients displayed activation of the TIM-3/galectin-9 signaling pathway. A similar finding was reported for lung adenocarcinoma patients [19]. Nevertheless, increased galectin-9⁺ dendritic-like macrophages have been correlated with prolonged survival and ACT benefit in stage IV melanoma patients [20]. These results suggest that this subpopulation plays a crucial role in carcinogenesis. However, the role of this subpopulation and its specific immune contexture in MIBC remains unknown.

In this study, we detected the frequency of Gal-9⁺TAMs in MIBC patients, evaluated their prognostic potential and assessed the predictive value of postoperative platinum-based adjuvant chemotherapy in this subpopulation. We also explored the specific immune contexture with different levels of Gal-9⁺ macrophage infiltration to clarify their effects on the tumor-immune microenvironment.

Materials and methods

Study population

This study began with a cohort of 215 consecutive patients who underwent radical cystectomy from 2002 to 2014 in the Zhongshan Hospital of Fudan University. Standard lymph node dissections were performed as part of radical cystectomy. Nodal tissues up to the common iliac bifurcation, lateral to the genitofemoral nerves, were removed, including the bilateral internal iliac, presacral, obturator fossa, and external iliac nodes. The following criteria were used: (1) no comorbidities; (2) follow-up information available; (3) pT ≥ 2 ; (4) postoperative histopathological diagnosis of MIBC; (5) treatment-naïve and no distant metastasis before surgery. Only 142 of 215 patients in this cohort were pathologically diagnosed with MIBC and enrolled for further analysis, including the assessment of the tissue microarrays (TMAs) constructed by Shanghai Outdo Biotech Co. Ltd. After immunohistochemistry, data for one patient were lost due to detachment. Thus, the final sample comprised 141 patients. After surgery, eligible patients received at least



one cycle of platinum-based chemotherapy: gemcitabine/cisplatin or methotrexate/vinblastine/adriamycin/cisplatin (MVAC). Indications for ACT were changed during the long time span (2002–2014) of the study. From 2002 to 2013, the indication was pT2+ patients, either with lymphovascular invasion (LVI) or high grades or pN+ disease, as based on hospital archives. From 2014 to the end of the study period, the indication was pT3+ or with pN+ disease or both. OS and RFS were defined as the time from surgery to death from all causes and recurrence, respectively, or to the most recent follow-up. During the follow-up period, physical examination and laboratory assessments (abdominal ultrasound or CT scan, chest imaging and urine cytology) were routinely performed every 3 months during the first year, semi-annually in the second year, and annually thereafter. The follow-up information was updated until July 2016, and the median follow-up was 56 months.

We evaluated 20 tumor and 6 paired peritumor specimens from MIBC patients who underwent radical cystectomy in the Shanghai Cancer Center from June 2018 to October 2018. Patients enrolled were treatment naïve before surgery (detailed information in Supplementary Fig. 1a).

Immunohistochemistry

Microarray development and single-staining were performed according to our previously described methods [21, 22]. Single-staining was performed on CD8⁺T cells, B cells, mast cells, Treg cells, NK cells and neutrophils. Double staining was performed on DCs, Th1 cells, Th2 cells and Gal-9⁺TAMs. Specific information on antibodies is detailed in Supplementary Table 4.

For dual immunohistochemistry, the TMA slides were dewaxed in a dry-heat oven, treated with xylene and graded alcohol and then washed three times with phosphate-buffered saline. After the slides were heated in sodium citrate buffer (0.01 M sodium citrate buffer, pH=6) for antigen retrieval, endogenous peroxidase was inhibited by adding 3% H₂O₂ for 30 min at 37 °C. The slides were then treated with 10% normal goat serum blocking solution for 45 min at 37 °C. Next, the sections were incubated with the first primary antibody for 2 h and subsequently washed. After adding the secondary horseradish peroxidase (HRP)-labeled antibody (goat anti-rabbit IgG) for 30 min, the diaminobenzidine (DAB) detection system was used to detect staining. The samples were then washed and incubated with second primary antibody overnight in a wet chamber at 4 °C. The next day, TMAs were washed and incubated with the secondary alkaline phosphatase (AP)-labeled (goat anti-mouse IgG) antibody in blocking buffer for 1 h at room temperature. Substrate working solution was prepared with 5 ml 100–200 mM Tris–hydrochloric acid (HCl) (pH 8.2–8.5), 80 µl reagent 1, 80 µl reagent 2 and 45 µl reagent 3, as

Fig. 2 Gal-9⁺TAMs show superior prediction abilities for the survival of MIBC patients. OS (left) and RFS (right) curves for **a, b** TAMs, **c, d** Gal-9⁻TAMs and **e, f** Gal-9⁺TAMs. **g, h** Prognostic effect of the frequency of Gal-9⁺TAMs compared to TAMs and Gal-9⁻TAMs for OS (left) and RFS (right). Forest plots show HRs (blue and red squares) and confidence intervals (horizontal ranges) derived from univariate and multivariate Cox regression analyses

instructed (VECTOR Blue Substrate kit). The sample was gently shaken for 20 min in the dark, after which the sections were washed, dehydrated, mounted and observed.

All slides were analyzed with a Leica DM6000 B microscope (Leica Microsystems). The number of immune cells was determined with Image-Pro Plus software (Media Cybernetics Inc.), and mean values from three respective areas (200× magnification) were recorded. All quantification was performed by two independent pathologists in a blind manner. The median cut-off values were 25%, 62%, and 62/HPF for Gal-9⁺TAMs, Gal-9⁻TAMs and TAMs, respectively.

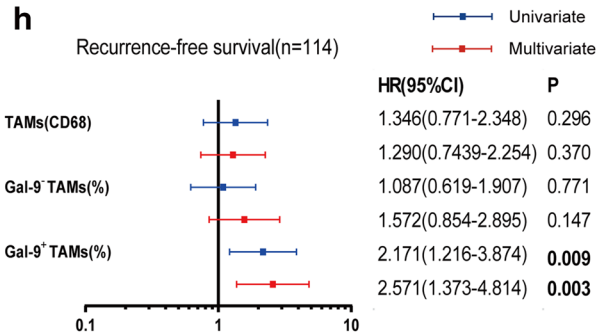
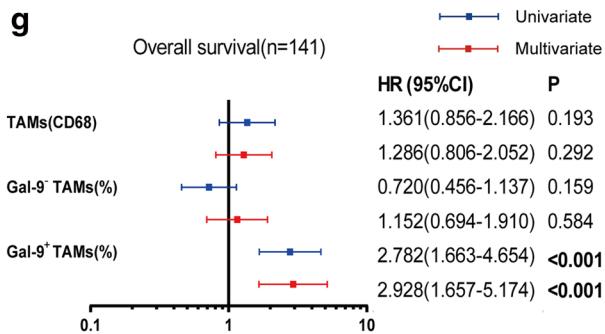
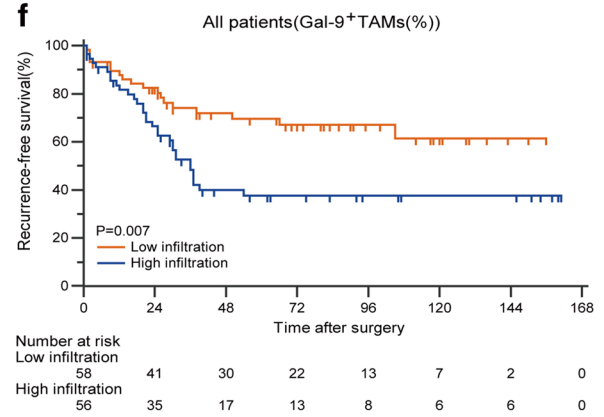
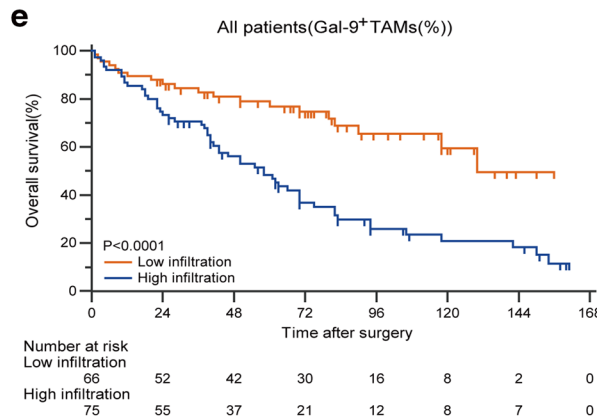
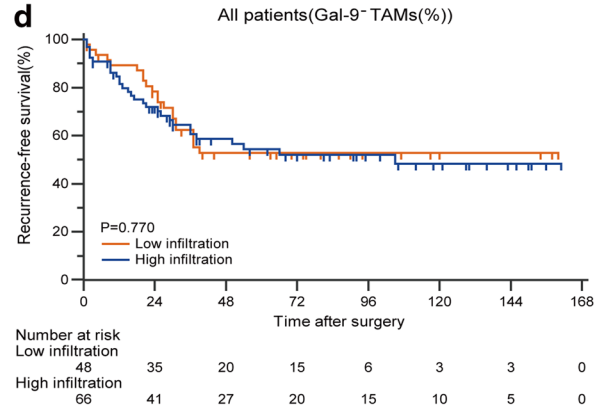
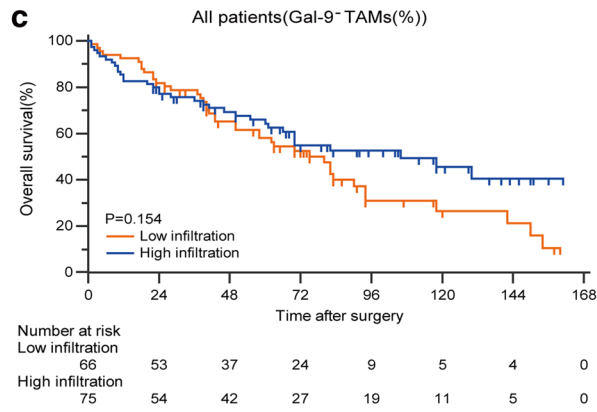
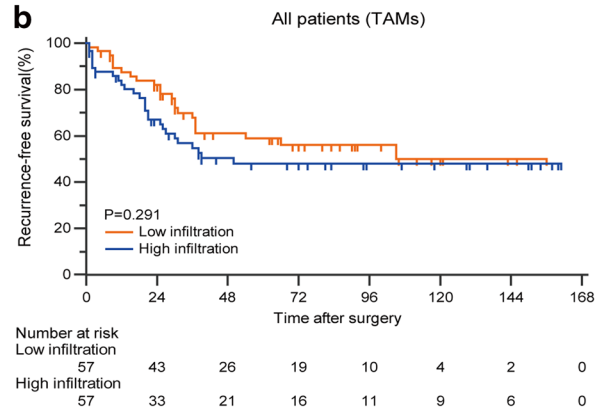
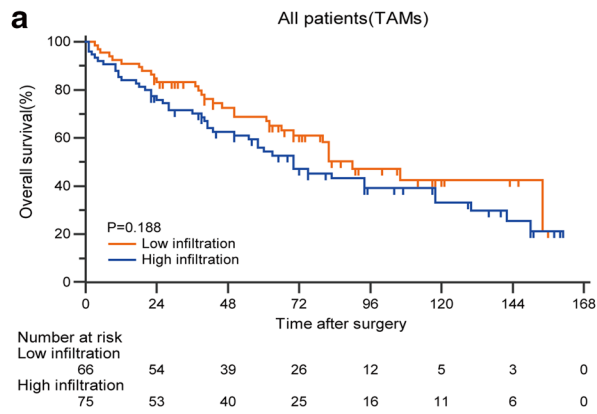
Flow cytometry

Human tissues (Supplementary Fig. 1a) were collected in Dulbecco's balanced salt solution (DBSS, Gibco) after radical cystectomy. Tumor and peritumor tissues were digested using collagenase IV and 10% FBS for 2 h at 37 °C, and a sample of approximately 1 × 10⁶ cells was centrifuged and incubated in RBC lysis buffer on ice for 5 min. Cells were incubated with Human Fc receptor block (BD Pharmingen) and stained for 30 min in the dark at 4 °C for surface markers. To evaluate intracellular cytokines, surface-stained cells were fixed and permeabilized with the Fixation/Permeabilization Solution Kit (BD Biosciences) for 30 min at 4 °C before intracellular staining. Transcription factor staining (FOXP3) was performed using a True-Nuclear transcription factor buffer set (Biolegend) according to the manufacturer's instructions. Cells were analyzed with a FACS Celesta flow cytometer (BD Biosciences), and data were analyzed by FlowJo V10 (TreeStar).

Cells were stained for the following markers: CD8⁺T cells (CD45⁺CD3⁺CD8⁺), CD4⁺T cells (CD45⁺CD3⁺CD4⁺), Treg cells (CD45⁺CD4⁺CD25⁺FOXP3⁺), NK cells (CD45⁺CD3⁻CD56⁺), macrophages (CD11b⁺CD45⁺CD68⁺) and tumor cells (CD45⁻EpCAM⁺). Dead cells were excluded by staining with Fixable Viability Stain 510. The specific markers are listed in Supplementary Table 5.

Statistical analysis

Categorical variables were analyzed by the χ^2 or Fisher's exact test, and continuous variables between different groups were assessed by *t* tests. Subgroup survival curves



were calculated by the Kaplan–Meier method and compared with the log rank test. Univariate and multivariate analyses were used to determine the hazard ratios (HR, 95% confidence interval) of clinico-pathological characteristics (Supplementary Table 1), ACT effectiveness and independent prognostic factors. The number of tumor-infiltrating immune cells and their surface markers or effector molecules were compared between two groups by Student's *t* test or the Mann–Whitney *U* test or among three groups by a non-parametric Kruskal–Wallis test and one-way ANOVA. Correlation among tumor-infiltrating immune cells was assessed using Spearman's correlation test. All grouped data are presented as the mean \pm SEM with significance indicated (*, for $p < 0.05$, **, for $p < 0.01$, ***, for $p < 0.001$; ns, no significance). All tests were two sided. Graphical and statistical analyses were performed using GraphPad Prism Software (version 7.00) and IBM SPSS Statistics software (Version 21).

Results

High levels of Gal-9⁺TAMs are associated with disease progression

To determine whether macrophages expressed galectin-9 in the tumor environment, we first evaluated the percentage level of Gal-9⁺TAMs from MIBC tissue samples by flow cytometry (FCM) (Fig. 1a). Compared to peritumor tissues, tumor tissues had a higher percentage of macrophages expressing galectin-9 (Fig. 1b). We also used immunohistochemistry to confirm this observation in a large tumor microarray from the Zhongshan cohort. Dual staining revealed that approximately 30% of TAMs expressed galectin-9 (Fig. 1c, d). Additionally, we utilized pathologic stage, grade and lymph node metastasis as covariables to gain further insight into the relationship between Gal-9⁺TAMs and disease progression. We found an increased frequency of Gal-9⁺TAMs with clinical stage (T2–T4) or grade (low–high) development in both fresh MIBC specimens and TMAs (Fig. 1e, f). Additionally, more Gal-9⁺TAMs accumulated in tumor tissues with a higher node stage (N1+) than in those with a lower stage (Supplementary Fig. 1b). These data suggest that Gal-9⁺TAMs are present in MIBC and are correlated with tumor progression.

Gal-9⁺TAMs exhibit superior prognostic abilities in MIBC

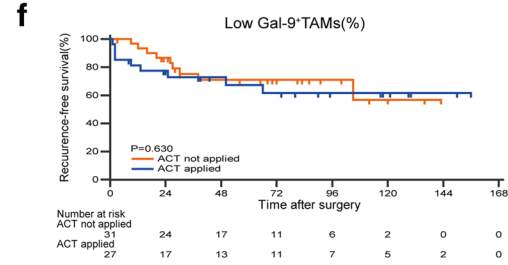
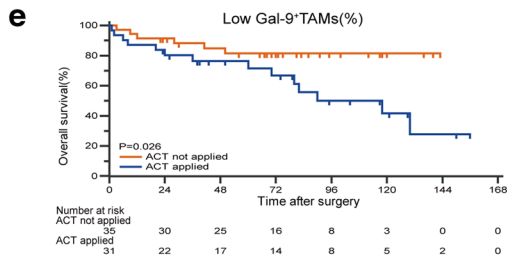
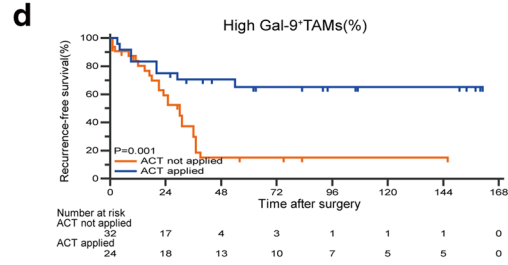
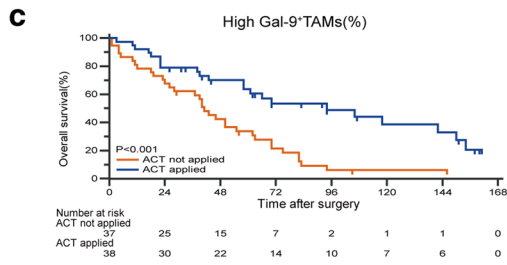
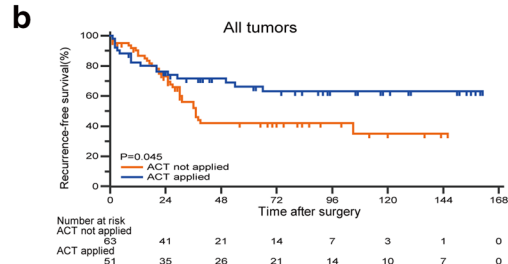
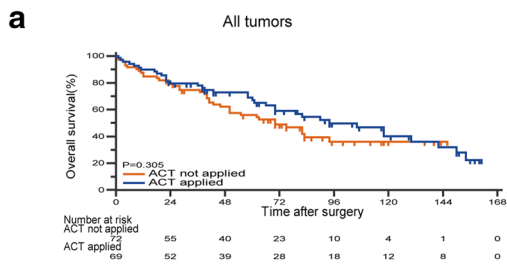
After confirming the existence of Gal-9⁺TAMs, we investigated whether this subpopulation was associated with clinical outcomes. We conducted Kaplan–Meier analysis of total macrophages and percentages of Gal-9⁺TAMs

Fig. 3 Patients with high-Gal-9⁺TAMs exhibit prominent adjuvant chemotherapy effectiveness. Kaplan–Meier analyses for OS and RFS of **a, b** all patients, **c, d** high-Gal-9⁺TAM patients and **e, f** low-Gal-9⁺TAM patients with or without ACT. Univariate and multivariate Cox regression analyses for ACT benefit on **g** OS and **h** RFS among different clinico-pathological variables

and Gal-9⁺TAMs. Patient characteristics and correlations with these populations are provided in Supplementary Table 2. Gal-9⁺TAMs, Gal-9[−]TAMs and TAMs ranged from 0 to 89%, 11 to 100% and 2 to 333 (200 \times magnification), respectively. Patients with high (≥ 62 /HPF) versus low (< 62 /HPF) TAM level, with high ($\geq 25\%$) versus low ($< 25\%$) Gal-9⁺TAM percentage level and with high ($\geq 62\%$) versus low ($< 62\%$) Gal-9[−]TAM percentage level were defined according to median cut-off values. The results showed no differences in OS or RFS for patients with high or low TAMs (Fig. 2a, b). Similarly, the percentages of Gal-9[−]TAMs could not stratify prognostic groups in either OS or RFS (Fig. 2c, d) curves. Only high frequencies of Gal-9⁺TAMs were significantly associated with worse OS and RFS (Fig. 2e, f) ($p < 0.0001$ and $p = 0.007$, respectively). Univariate and multivariate Cox regression analyses (Fig. 2g, h) indicated that a dense subpopulation of Gal-9⁺TAMs, but not TAMs or Gal-9[−]TAMs, was significantly correlated with poor prognosis (Supplementary Table 3). This finding suggests that a high percentage of Gal-9⁺TAMs may discriminate prognostic groups and could be an independent prognostic factor for MIBC patients.

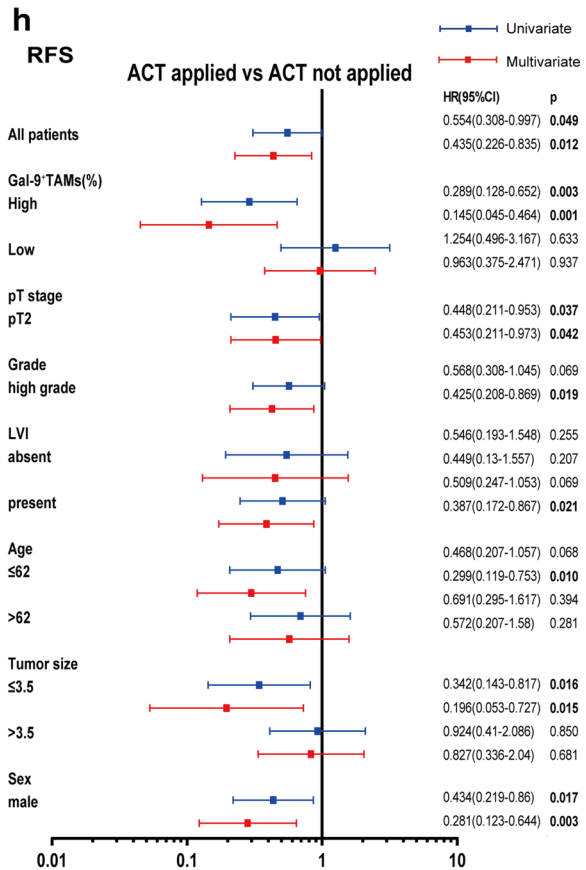
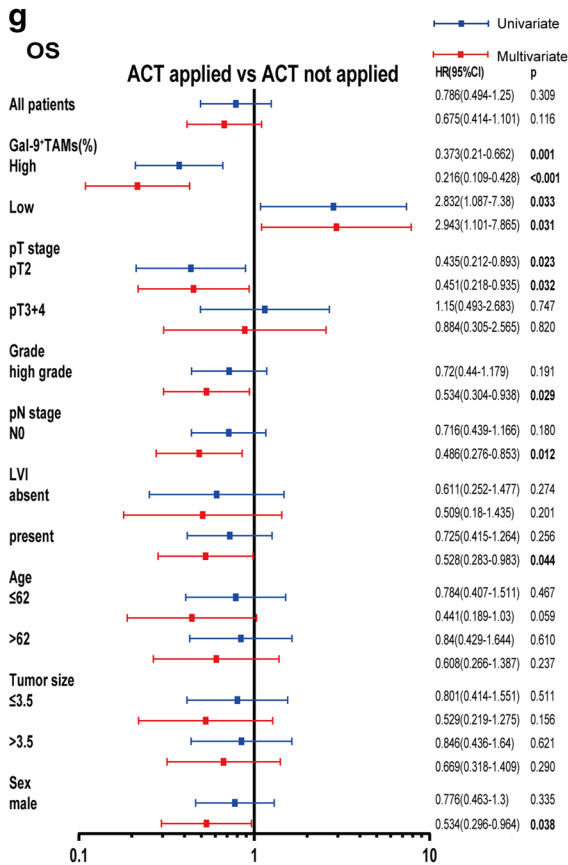
Patients with high Gal-9⁺TAMs show survival benefit from postoperative adjuvant chemotherapy

Because post-surgery ACT is universal in the clinical management of MIBC, we evaluated the efficacy of ACT in patients with different Gal-9⁺TAM percentage level. ACT did not prolong OS (Fig. 3a) but did prolong RFS (Fig. 3b) in the Zhongshan cohort. Interestingly, after separating patients into two groups, we found that ACT strongly enhanced OS ($p < 0.001$, Fig. 3c) and RFS ($p = 0.001$, Fig. 3d) in the high Gal-9⁺TAM group. Conversely, patients in the low-infiltration group acquired no OS (Fig. 3e) or RFS (Fig. 3f) survival benefit. A test for the interaction between different levels of Gal-9⁺TAMs and ACT revealed that the benefit in patients with high level of Gal-9⁺TAMs was superior to that in the low-infiltration group. In addition, we explored the benefit of ACT on OS (Fig. 3g) and RFS (Fig. 3h) in different subgroups of MIBC patients according to clinical–pathological variables. ACT prolonged OS of male patients and patients with pT2 stage, high grade, pN0, or LVI absent. ACT also prolonged RFS in male patients and patients with pT2 stage,



P<0.001
for
interaction

P=0.019
for
interaction



high grade, or LVI absent, as well as patients ≤ 62 years, or whose tumors were ≤ 3.5 cm. Moreover, the optimal effectiveness of ACT for both OS (univariate: HR 0.373, 95% confidence interval 0.210–0.662, $p=0.001$; multivariate: HR 0.216, 95% confidence interval 0.109–0.428, $p<0.001$) and RFS (univariate: HR 0.289, 95% confidence interval 0.128–0.652, $p=0.003$; multivariate: HR 0.145, 95% confidence interval 0.045–0.464, $p=0.001$) correlated with high Gal-9⁺TAM level. Taken together, these findings demonstrate survival benefits after postoperative ACT among patients in the high-Gal-9⁺TAM group, whereas patients in the low-Gal-9⁺TAM group showed no benefit.

Dynamic changes of immune cell infiltration with different levels of Gal-9⁺TAMs

Our previous results demonstrated that Gal-9⁺TAMs could predict the prognosis for MIBC patients. Immune contexture delineated the morphologic and functional orientation of tumor-infiltrating immune cells, which were closely linked to patient outcomes [23]. Therefore, we examined the relationship between Gal-9⁺TAMs and their specific immune contexture. We used IHC to assess nine major tumor-infiltrating immune cells from the Zhongshan cohort and observed that patients in the high-Gal-9⁺TAM group had increased Treg and mast cells and reduced counts of CD8⁺T and DC cells (Fig. 4a–d). No significant differences of other infiltrating immune cells between the two groups were observed (Fig. 4e–i). We generated a heat map to illustrate the Spearman's correlations between different cell types and Gal-9⁺TAMs or total TAMs (Fig. 4j and Supplementary Table 6), highlighting that Gal-9⁺TAMs were negatively associated with CD8⁺T and DC cells and positively associated with mast and Treg cells. Additionally, total TAMs were positively associated with Treg cells, B cells and neutrophils (Supplementary Table 6). Given that CD8⁺T cells and dendritic cells are known to play important roles in antitumor immunity and that Treg cells are associated with pro-tumoral immunity, our data imply that increased levels of Gal-9⁺TAMs are likely correlated with a pro-tumorigenic immune contexture in MIBC patients.

High Gal-9⁺TAMs are associated with the immunosuppressive microenvironment and active proliferation of tumor cells

To explore the association between Gal-9⁺TAMs and particular immune activities or functions, we investigated immune cytotoxic molecules (IFN- γ , granzyme B (GZMB), perforin 1 (PRF1)), immunosuppressive molecules (IL-10, TGF- β), and immune checkpoint molecules (PD-1, TIM-3, CTLA-4, T-cell Ig and ITIM domain (TIGIT), LAG-3) expressed or secreted by immune cells (Fig. 5a). We also

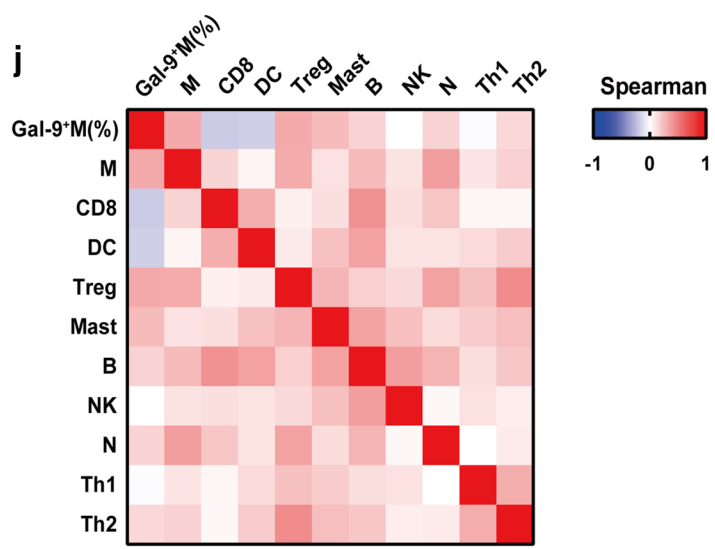
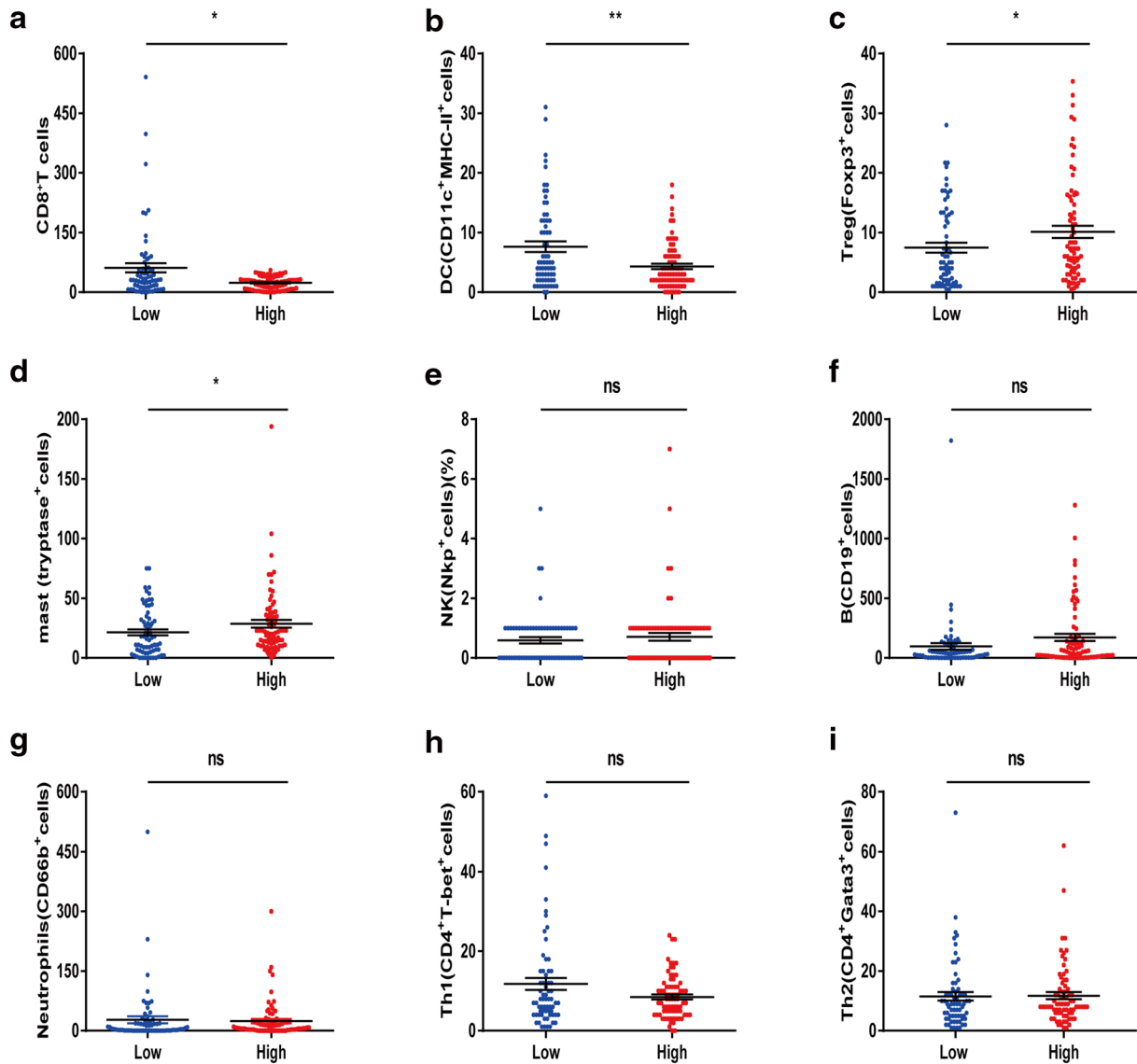
Fig. 4 Gal-9⁺TAMs, but not total TAMs, are negatively associated with CD8⁺T cells and dendritic cells and positively associated with mast and Treg cells between the high- and low-infiltration group. Comparison of **a** CD8⁺T cells, **b** DC cells, **c** Treg cells, **d** mast cells, **e** NK cells, **f** B cells, **g** neutrophils, **h** Th1 cells and **i** Th2 cells with high or low Gal-9⁺TAMs. **j** Heat map illustrating Spearman's correlation of eleven immune cells. *M* TAMs

assessed proliferation and apoptosis of tumor cells from fresh tumor tissues. In the high-Gal-9⁺TAM group, CD45⁺ cells secreted less IFN- γ , GZMB, and PRF1 and more IL-10 and TGF β , and had enhanced levels of PD-1 and TIM-3. In the high-Gal-9⁺TAM group, CD8⁺ T cells had decreased effector molecules and upregulated immune checkpoints. The number of PD-1⁺TIM-3⁺CD8⁺T cells, known as exhausted T cells, was also significantly elevated. Less IFN- γ was secreted by conventional CD4⁺T cells and more IL-10 and TGF- β were secreted by Treg cells. When we examined NK cells, with the exception of decreased GZMB in the high-infiltration group, neither cell counts nor functions were different between the two groups. Intriguingly, active proliferation of tumor cells was detected via Ki67 staining in the high-infiltration group. However, tumor cell apoptosis did not differ between the two groups (Fig. 5b, c). In summary, dynamic interactions between Gal-9⁺TAMs and immune cells, as well as between Gal-9⁺TAMs and tumor cells, indicated a suppressive tumor-immune microenvironment in MIBC patients. The graphical abstract of this study is shown in Fig. 6.

Discussion

Galectin-9, a type of tandem-repeat galectin, is believed to play a role in tumor biology. This protein exhibits multifaceted functions [24], such as in cell cycle control, apoptosis, immune escape and tumor angiogenesis, indicating that it can be a therapeutic target in cancer treatments. Gal-9⁺ macrophages display dichotomous roles in tumor growth and metastasis in several cancers [18, 20, 25]. Nevertheless, little is known about its role in MIBC.

We found variable galectin-9 expression by tumor-associated macrophages in MIBC patients, and its frequency increased with disease progression. The infiltration level of Gal-9⁺TAMs was significantly related to the survival of patients. In metastatic melanoma galectin-9 was observed to colocalize with pro-tumoral CD68⁺ macrophages [26] or CD206⁺ myeloid cells [27]; however, no significant relationship between the percentage of Gal-9⁺TAMs or TAMs and clinical outcomes was observed. These results suggest that Gal-9⁺TAMs might account for the poor outcome of some MIBC patients with high levels of TAMs. Thus, according to our results, galectin-9 expressed by macrophages may be a prognostic marker and a potential therapeutic target for MIBC.



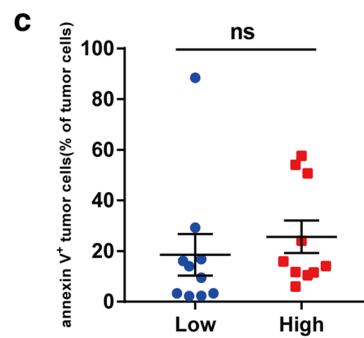
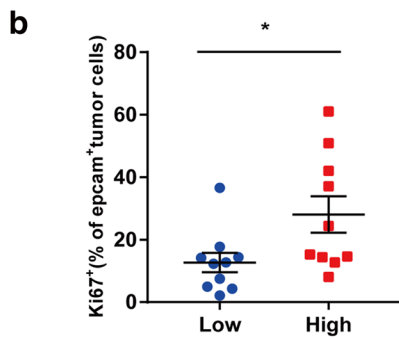
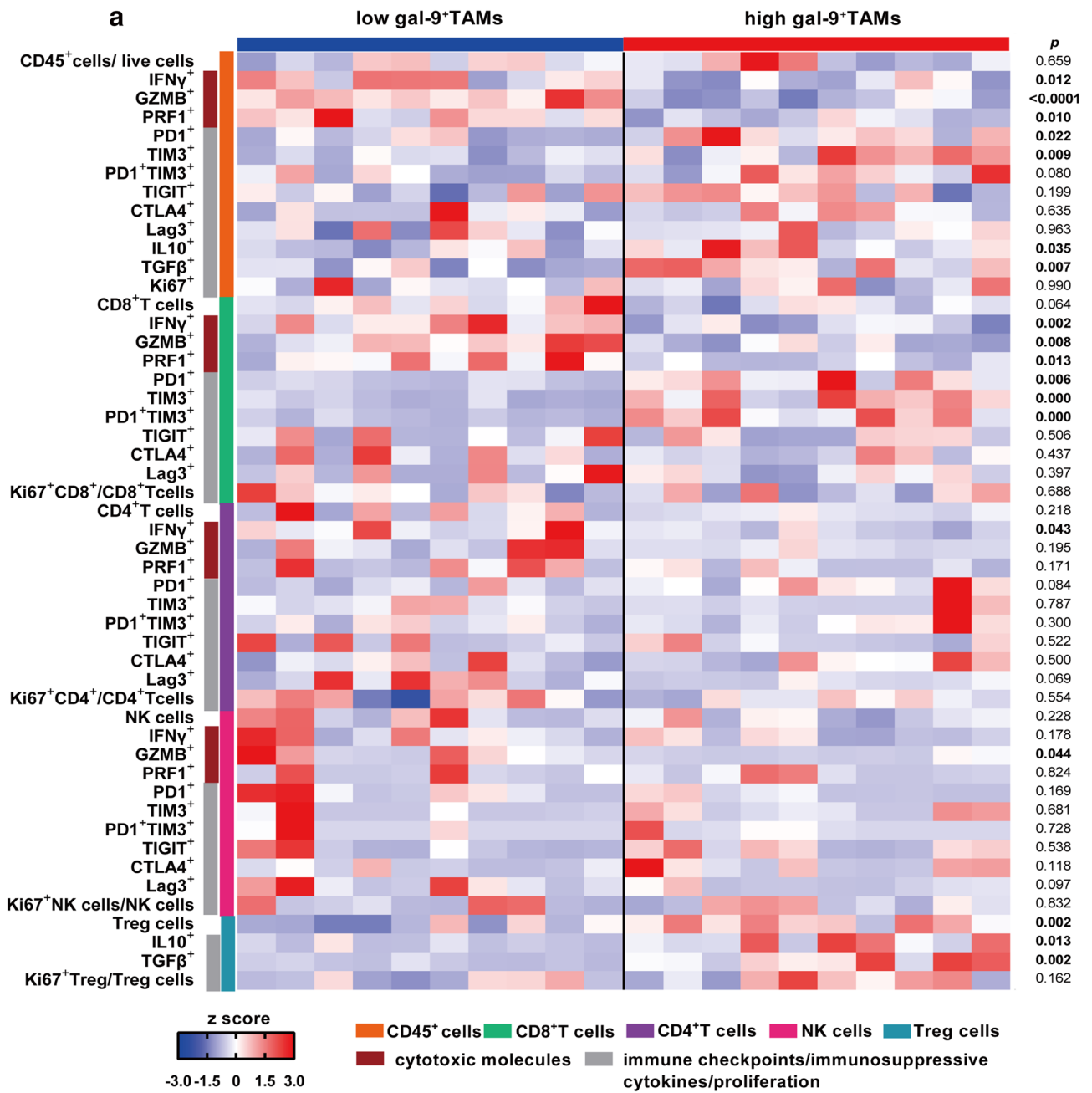


Fig. 5 High-Gal-9⁺TAMs are correlated with reduced cytotoxic molecules, enhanced immune checkpoint expression or secretion of immunosuppressive cytokines and active proliferation of tumor cells. **a** Flow cytometry-generated heat map of cytotoxic markers (IFN- γ , GZMB, PRF1), immune checkpoint molecules (PD-1, TIM-3, CTLA-4, TIGIT, Lag-3) and immunosuppressive cytokines (IL-10, TGF- β) of CD45⁺, CD8⁺T, CD4⁺T, NK and Treg cells from MIBC samples with high ($n=10$) and low ($n=10$) Gal-9⁺TAM levels. All populations are a fraction of the total CD45⁺ immune cells, unless otherwise noted. Data for each row are normalized as Z score; each column shows data from one person. **b** and **c** Ki67 (left) and annexin V (right) staining of tumor cells between high ($n=10$) and low ($n=10$) Gal-9⁺TAM groups

Some efforts have been made to chart the immune landscape, portray the functional states of immune cells and integrate immune cell-, tumor cell- and microenvironment-associated parameters with clinical outcomes and the effects of chemotherapies, immunotherapies and other therapeutic regimens [12, 23, 28–31]. These studies attempted to delineate the composition and distribution of CD8⁺T cells, DC cells, Treg cells, mast cells and other immune cells, linking these immune contexts to disease prognosis. Briefly, CD8⁺T, dendritic, Treg and mast cells are associated with patient survival [10, 22, 32–34] in bladder cancer. In both OS and RFS analyses, we found that patients with high infiltration of Gal-9⁺TAMs had significant survival benefits from ACT. To further explore the related mechanisms, we applied IHC to detect nine major immune cells within TMAs from

the Zhongshan cohort and found increased infiltration of Treg and mast cells and decreased infiltration of CD8⁺T and DC cells among MIBC patients in the high-Gal-9⁺TAM groups. These findings are consistent with our previous study in which advanced MIBC patients whose immunotypes were CTL^{low}NK^{low}Treg^{high}Macrophage^{high}Mast cell^{high} had a better response to postoperative ACT but with a worse 5-year OS [20].

A previous study [35] verified that gemcitabine treatments shifted the phenotype of TAMs from pro-tumor to anti-tumor, indicating that the presence of TAMs was important for ACT. Another study showed the ability of galectin-9 to strengthen TLRs in inflammatory reactions [36], indicating that its presence might result in enhanced chemotherapy efficacy [37]. Therefore, determination of the Gal-9⁺TAM content might help select patients who are appropriate for ACT.

PD-1 inhibitors have been approved by the FDA for targeted therapy of bladder cancer [38, 39], indicating the therapeutic potential of immune inhibitors. To correlate our research with these clinical applications, we analyzed MIBC tumors for the expression of key immune-associated molecules by flow cytometric analysis. Our results showed increased leukocyte expression of immune checkpoint molecules and decreased cytotoxic molecules in the high-Gal-9⁺TAM group, suggestive of an immunosuppressive microenvironment. Despite the decrease in CD8⁺T-cell infiltration

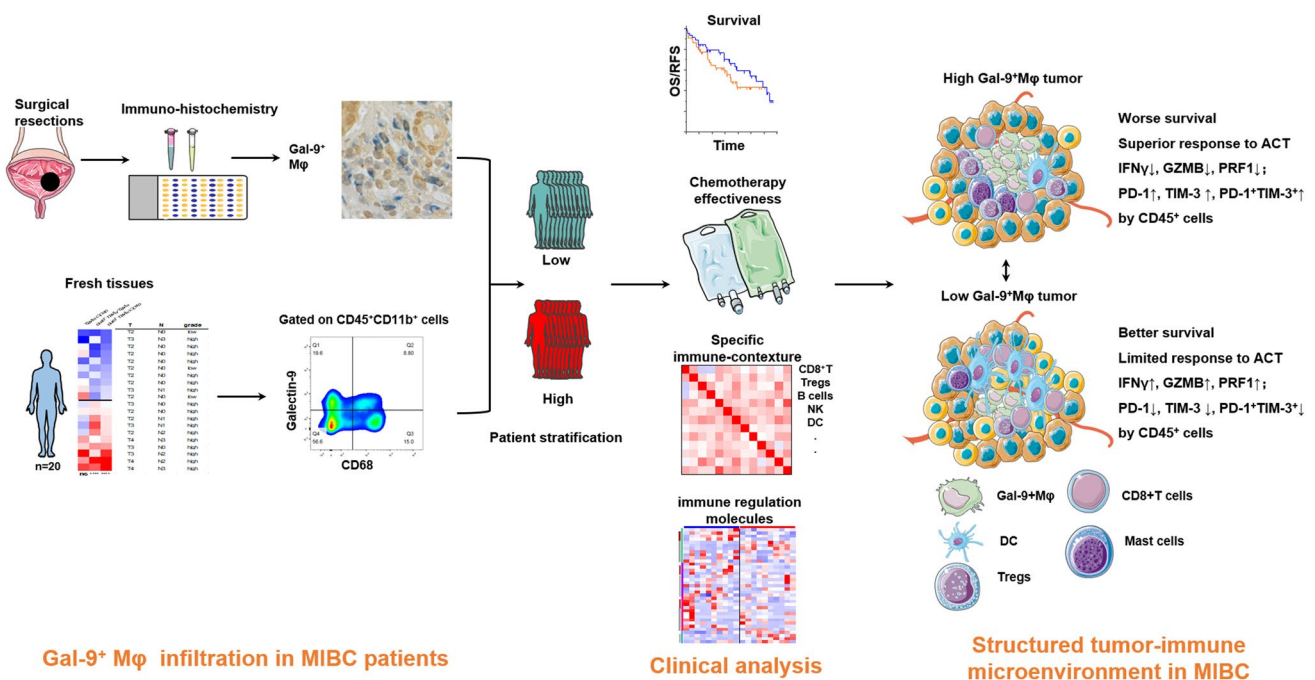


Fig. 6 Model depicting the structured tumor-immune microenvironment in MIBC patients with the infiltration of Gal-9⁺TAMs. As demonstrated in patients with high or low Gal-9⁺TAM level, we explore

survival curves, chemotherapy effectiveness, specific immune contexture and immune regulation molecules. Two patterns of structured tumor-immune microenvironment are illustrated

in patients with high Gal-9⁺TAMs, the CD8⁺T cells in these patients had higher levels of the exhaustion markers, PD-1 and TIM-3. PD-1⁺ or TIM-3⁺ leukocytes also accumulated in the high-infiltration group. Because exhausted T cells can be reinvigorated by PD-1 blockade [40] and TIM-3 inhibitors have already been tested in several clinical trials, the combined use of multiple immuno-oncology checkpoint inhibitors is a good strategy that is increasingly being tested in bladder cancer [41]. Therefore, our findings suggest that patients with high infiltration of Gal-9⁺TAMs are likely to benefit from PD-1 inhibitors or combined therapy (PD-1 inhibitors + chemotherapeutic drugs). This therapy was tested in a recent clinical trial (NCT01524991) and the results showed that patients with metastatic urothelial cancer had a high response rate (approximately 64%) to combination agents (gemcitabine + cisplatin + ipilimumab) [42].

However, there are still some limitations. First, the design was retrospective, the number of patients was relatively small, and the study was conducted at only one clinical center. An external cohort is needed to confirm the correlation between Gal-9⁺TAMs and prognosis of post-surgery ACT. In addition, galectin-9 is differentially expressed within or on the surface of various cell types. In this study, we did not take the effects of Gal-9⁺ tumor cells, Gal-9⁺ endothelial cells or other cells expressing galectin-9 on tumor immunity and therapy into account. Thus, more thorough studies of these cells are needed to elucidate the biological function of galectin-9 in MIBC.

Conclusions

Our study confirms the existence of Gal-9⁺TAMs in MIBC and demonstrates that patients with increased infiltration of Gal-9⁺TAMs have a worse prognosis but can obtain a survival benefit from adjuvant chemotherapy. High Gal-9⁺TAM level corresponds to a pro-tumorigenic immune contexture and has a strong positive correlation with PD-1⁺TIM-3⁺CD8⁺ exhausted T cells, which might support the use of combination therapy (chemotherapy and immunotherapy) for these patients.

Author contributions YQ, YC, ZW and LC contributed to the acquisition, analysis and interpretation of data, statistical analysis and drafting of the manuscript. YK, PZ, ZL, QZ, YC, JW, QB, YX, LL, YZ, LX, BD and JG provided technical and material support; YW, WZ and JX were responsible for the study concept and design, analysis and interpretation of data, drafting of the manuscript, obtaining funding and study supervision. All authors read and approved the final manuscript.

Funding This study was funded by grants from the National Natural Science Foundation of China (81671628, 31770851, 81702496, 81702497, 81702805, 81772696, 81871306, 81872082, 81902556,

81902563, 81902898, 81974393), the National Key R&D Program of China (2017YFC0114303), the Shanghai Municipal Natural Science Foundation (16ZR1406500, 17ZR1405100, 19ZR1431800), the Guide Project of Science and Technology Commission of Shanghai Municipality (17411963100), the Shanghai Sailing Program (18YF1404500, 19YF1407900, 19YF1427200), the Shanghai Municipal Commission of Health and Family Planning Program (20174Y0042, 201840168, 20184Y0151), the Fudan University Shanghai Cancer Center for Outstanding Youth Scholars Foundation (YJYQ201802) and a grant from the Shanghai Cancer Research Charity Center. None of the study sponsors contributed to the study design, or the collection, analysis or interpretation of data.

Compliance with ethical standards

Conflict of interest The authors declare they have no conflict of interest.

Ethics approval and ethical standards This study was approved by the Clinical Research Ethics Committee of Zhongshan Hospital, Fudan University (No. B2015-030) and the institutional review board and the ethics committee of Shanghai Cancer Center, Fudan University (No. 050432-4-1212B). This study was performed following the ethical principles of the Helsinki Declaration.

Informed consent Patients from the Zhongshan hospital and the Shanghai Cancer Center signed informed consent forms before surgery that permitted the usage of specimens and clinical data for research and publication under the condition of anonymity.

References

1. (2019) 17th International Congress of Immunology (2019) Beijing, China. *Eur J Immunol* 49:1–2223. <https://doi.org/10.1002/eji.201970400>
2. Sanli O, Dobruch J, Knowles MA, Burger M, Alemozaffar M, Nielsen ME, Lotan Y (2017) Bladder cancer. *Nat Rev Dis Primers* 3:17022. <https://doi.org/10.1038/nrdp.2017.22>
3. Alfred Witjes J, Lebrecht T, Comperat EM et al (2017) Updated 2016 EAU guidelines on muscle-invasive and metastatic bladder cancer. *Eur Urol* 71:462–475. <https://doi.org/10.1016/j.eururo.2016.06.020>
4. Chen DS, Mellman I (2017) Elements of cancer immunity and the cancer-immune set point. *Nature* 541:321–330. <https://doi.org/10.1038/nature21349>
5. Spiess PE, Agarwal N, Bangs R et al (2017) Bladder cancer, version 5.2017, NCCN clinical practice guidelines in oncology. *J Natl Compr Cancer Netw* 15:1240–1267. <https://doi.org/10.6004/jcncc.2017.0156>
6. Zibelman M, Ramamurthy C, Plimack ER (2016) Emerging role of immunotherapy in urothelial carcinoma-advanced disease. *Urol Oncol* 34:538–547. <https://doi.org/10.1016/j.urolonc.2016.10.017>
7. Sjobahl G, Lovgren K, Lauss M et al (2014) Infiltration of CD3(+) and CD68(+) cells in bladder cancer is subtype specific and affects the outcome of patients with muscle-invasive tumors. *Urol Oncol* 32:791–797. <https://doi.org/10.1016/j.urolonc.2014.02.007>
8. Sica A, Schioppa T, Mantovani A, Allavena P (2006) Tumour-associated macrophages are a distinct M2 polarised population promoting tumour progression: potential targets of anti-cancer therapy. *Eur J Cancer* 42:717–727. <https://doi.org/10.1016/j.ejca.2006.01.003>

9. Ichimura T, Morikawa T, Kawai T et al (2014) Prognostic significance of CD204-positive macrophages in upper urinary tract cancer. *Ann Surg Oncol* 21:2105–2112. <https://doi.org/10.1245/s10434-014-3503-2>
10. Fridman WH, Zitvogel L, Sautes-Fridman C, Kroemer G (2017) The immune contexture in cancer prognosis and treatment. *Nat Rev Clin Oncol* 14:717–734. <https://doi.org/10.1038/nrcli.nonc.2017.101>
11. Helm O, Held-Feindt J, Grage-Griebenow E et al (2014) Tumor-associated macrophages exhibit pro- and anti-inflammatory properties by which they impact on pancreatic tumorigenesis. *Int J Cancer* 135:843–861. <https://doi.org/10.1002/ijc.28736>
12. Fridman WH, Pages F, Sautes-Fridman C, Galon J (2012) The immune contexture in human tumours: impact on clinical outcome. *Nat Rev Cancer* 12:298–306. <https://doi.org/10.1038/nrc3245>
13. Irie A, Yamauchi A, Kontani K et al (2005) Galectin-9 as a prognostic factor with antimetastatic potential in breast cancer. *Clin Cancer Res* 11:2962–2968. <https://doi.org/10.1158/1078-0432.ccr-04-0861>
14. Choi SI, Seo KW, Kook MC, Kim CG, Kim YW, Cho SJ (2017) Prognostic value of tumoral expression of galectin-9 in gastric cancer. *Turk J Gastroenterol* 28:166–170. <https://doi.org/10.5152/tjg.2017.16346>
15. Wang Y, Sun J, Ma C et al (2016) Reduced expression of Galectin-9 contributes to a poor outcome in colon cancer by inhibiting NK cell chemotaxis partially through the Rho/ROCK1 signaling pathway. *PLoS One* 11:e0152599. <https://doi.org/10.1371/journal.pone.0152599>
16. Sideras K, Biermann K, Verheij J et al (2017) PD-L1, Galectin-9 and CD8+ tumor-infiltrating lymphocytes are associated with survival in hepatocellular carcinoma. *OncoImmunology* 6:e1273309. <https://doi.org/10.1080/2162402X.2016.1273309>
17. Liu Y, Liu Z, Fu Q, Wang Z, Fu H, Liu W, Wang Y, Xu J (2017) Galectin-9 as a prognostic and predictive biomarker in bladder urothelial carcinoma. *Urol Oncol* 35:349–355. <https://doi.org/10.1016/j.urolonc.2017.02.008>
18. Li H, Wu K, Tao K et al (2012) Tim-3/galectin-9 signaling pathway mediates T-cell dysfunction and predicts poor prognosis in patients with hepatitis B virus-associated hepatocellular carcinoma. *Hepatology* 56:1342–1351. <https://doi.org/10.1002/hep.25777>
19. Kratochvill F, Neale G, Haverkamp JM et al (2015) TNF counterbalances the emergence of M2 tumor macrophages. *Cell Rep* 12:1902–1914. <https://doi.org/10.1016/j.celrep.2015.08.033>
20. Melief SM, Visconti VV, Visser M et al (2017) Long-term survival and clinical benefit from adoptive T-cell transfer in Stage IV melanoma patients is determined by a four-parameter tumor immune signature. *Cancer Immunol Res* 5:170–179. <https://doi.org/10.1158/2326-6066.CIR-16-0288>
21. Fu H, Zhu Y, Wang Y et al (2018) Identification and validation of stromal immunotype predict survival and benefit from adjuvant chemotherapy in patients with muscle invasive bladder cancer. *Clin Cancer Res*. <https://doi.org/10.1158/1078-0432.ccr-17-2687>
22. Liu Z, Zhu Y, Xu L et al (2018) Tumor stroma-infiltrating mast cells predict prognosis and adjuvant chemotherapeutic benefits in patients with muscle invasive bladder cancer. *OncoImmunology* 7:e1474317. <https://doi.org/10.1080/2162402x.2018.1474317>
23. Becht E, Giraldo NA, Dieu-Nosjean MC, Sautes-Fridman C, Fridman WH (2016) Cancer immune contexture and immunotherapy. *Curr Opin Immunol* 39:7–13. <https://doi.org/10.1016/j.coi.2015.11.009>
24. Heusschen R, Griffioen AW, Thijssen VL (2013) Galectin-9 in tumor biology: a jack of multiple trades. *Biochim Biophys Acta* 1836:177–185. <https://doi.org/10.1016/j.bbcan.2013.04.006>
25. Ohue Y, Kurose K, Nozawa R et al (2016) Survival of lung adenocarcinoma patients predicted from expression of PD-L1, Galectin-9, and XAGE1 (GAGED2a) on tumor cells and tumor-infiltrating T cells. *Cancer Immunol Res* 4:1049–1060. <https://doi.org/10.1158/2326-6066.CIR-15-0266>
26. Enninga EA, Nevala WK, Holtan SG, Leontovich AA, Markovic SN (2016) Galectin-9 modulates immunity by promoting Th2/M2 differentiation and impacts survival in patients with metastatic melanoma. *Melanoma Res* 26:429–441. <https://doi.org/10.1097/CMR.0000000000000281>
27. Enninga EAL, Chatzopoulos K, Butterfield JT, Sutor SL, Leontovich AA, Nevala WK, Flotte TJ, Markovic SN (2018) CD206-positive myeloid cells bind galectin-9 and promote a tumor-supportive microenvironment. *J Pathol* 245:468–477. <https://doi.org/10.1002/path.5093>
28. Sotiriou C, Pusztai L (2009) Gene-expression signatures in breast cancer. *N Engl J Med* 360:790–800. <https://doi.org/10.1056/NEJMra0801289>
29. Keren L, Bosse M, Marquez D et al (2018) A Structured tumor-immune microenvironment in triple negative breast cancer revealed by multiplexed ion beam imaging. *Cell* 174(1373–87):e19. <https://doi.org/10.1016/j.cell.2018.08.039>
30. Galluzzi L, Buque A, Kepp O, Zitvogel L, Kroemer G (2015) Immunological effects of conventional chemotherapy and targeted anticancer agents. *Cancer Cell* 28:690–714. <https://doi.org/10.1016/j.ccell.2015.10.012>
31. Iwamoto T, Bianchini G, Booser D et al (2011) Gene pathways associated with prognosis and chemotherapy sensitivity in molecular subtypes of breast cancer. *J Natl Cancer Inst* 103:264–272. <https://doi.org/10.1093/jnci/djq524>
32. Ayari C, LaRue H, Hovington H, Decobert M, Harel F, Bergeron A, Tetu B, Lacombe L, Fradet Y (2009) Bladder tumor infiltrating mature dendritic cells and macrophages as predictors of response to bacillus Calmette-Guerin immunotherapy. *Eur Urol* 55:1386–1395. <https://doi.org/10.1016/j.eururo.2009.01.040>
33. Ayari C, LaRue H, Hovington H, Caron A, Bergeron A, Tetu B, Fradet V, Fradet Y (2013) High level of mature tumor-infiltrating dendritic cells predicts progression to muscle invasion in bladder cancer. *Hum Pathol* 44:1630–1637. <https://doi.org/10.1016/j.humpath.2013.01.014>
34. Winerdal ME, Marits P, Winerdal M, Hasan M, Rosenblatt R, Tolf A, Selling K, Sherif A, Winqvist O (2011) FOXP3 and survival in urinary bladder cancer. *BJU Int* 108:1672–1678. <https://doi.org/10.1111/j.1464-410X.2010.10020.x>
35. Di Caro G, Cortese N, Castino GF et al (2016) Dual prognostic significance of tumour-associated macrophages in human pancreatic adenocarcinoma treated or untreated with chemotherapy. *Gut* 65:1710–1720. <https://doi.org/10.1136/gutjnl-2015-309193>
36. Golden-Mason L, Rosen HR (2017) Galectin-9: diverse roles in hepatic immune homeostasis and inflammation. *Hepatology* 66:271–279. <https://doi.org/10.1002/hep.29106>
37. Apetoh L, Ghiringhelli F, Tesniere A et al (2007) Toll-like receptor 4-dependent contribution of the immune system to anticancer chemotherapy and radiotherapy. *Nat Med* 13:1050–1059. <https://doi.org/10.1038/nm1622>
38. Topalian SL, Hodi FS, Brahmer JR et al (2012) Safety, activity, and immune correlates of anti-PD-1 antibody in cancer. *N Engl J Med* 366:2443–2454. <https://doi.org/10.1056/NEJMoa1200690>
39. Sharma P, Callahan MK, Bono P et al (2016) Nivolumab monotherapy in recurrent metastatic urothelial carcinoma (CheckMate 032): a multicentre, open-label, two-stage, multi-arm, phase 1/2 trial. *Lancet Oncol* 17:1590–1598. [https://doi.org/10.1016/s1470-2045\(16\)30496-x](https://doi.org/10.1016/s1470-2045(16)30496-x)
40. Wherry EJ, Kurachi M (2015) Molecular and cellular insights into T cell exhaustion. *Nat Rev Immunol* 15:486. <https://doi.org/10.1038/nri3862>
41. Aitken M, Kleinrock M, Simorellis A, Nass D (2018) Global oncology trends 2018. Innovation, expansion and disruption.



IQVIA Institute for Human Data Science. Parsippany Google Scholar. <https://www.iqvia.com/institute/reports/global-oncology-trends-2018>. Accessed 24 May 2018

42. Galsky MD, Wang H, Hahn NM et al (2018) Phase 2 trial of gemcitabine, cisplatin, plus ipilimumab in patients with metastatic

urothelial cancer and impact of DNA damage response gene mutations on outcomes. *Eur Urol* 73:751–759

Publisher's Note Springer Nature remains neutral with regard to jurisdictional claims in published maps and institutional affiliations.

Affiliations

Yangyang Qi¹ · Yuan Chang² · Zewei Wang³ · Lingli Chen⁴ · Yunyi Kong⁵ · Peipei Zhang⁶ · Zheng Liu² · Quan Zhou⁷ · Yifan Chen¹ · Jiajun Wang³ · Qi Bai³ · Yu Xia³ · Li Liu³ · Yu Zhu² · Le Xu⁸ · Bo Dai² · Jianming Guo³ · Yiwei Wang⁹ · Jiejie Xu⁷  · Weijuan Zhang¹ 

✉ Yiwei Wang
wang.yiwei@sh9hospital.org

✉ Jiejie Xu
jjxufdu@fudan.edu.cn

✉ Weijuan Zhang
weijuanzhang@fudan.edu.cn

¹ Department of Immunology, School of Basic Medical Sciences, Fudan University, Building West 13, No. 138 Yixueyuan Road, Shanghai 200032, China

² Department of Urology, Fudan University Shanghai Cancer Center, Shanghai, China

³ Department of Urology, Zhongshan Hospital, Fudan University, Shanghai, China

⁴ Department of Pathology, Zhongshan Hospital, Fudan University, Shanghai, China

⁵ Department of Pathology, Fudan University Shanghai Cancer Center, Shanghai, China

⁶ Department of Pathology, Ruijin Hospital, Shanghai Jiao Tong University School of Medicine, Shanghai, China

⁷ Department of Biochemistry and Molecular Biology, School of Basic Medical Sciences, Fudan University, Building West 7, No. 138 Yixueyuan Road, Shanghai 200032, China

⁸ Department of Urology, Ruijin Hospital, Shanghai Jiao Tong University School of Medicine, Shanghai, China

⁹ Department of Urology, Shanghai Ninth People's Hospital, Shanghai Jiao Tong University School of Medicine, No. 639 Manufacturing Bureau Road, Shanghai 200011, China